SSC PACIFIC: APPLICATIONS IN NONLINEAR SCIENCES

Modeling Nonlinear Dynamics Systems

Dr. Patrick Longhini

SSC Pacific, Code 71730

Email longhini@spawar.navy.mil

SPAWAR
Systems Center
PACIFIC

Collaborators

SSC Pacific Team: Code 71730 & *71130

Dr. Visarath In
Dr. Adi Bulsara
Dr. Joseph Neff
Anna Leese de Escobar*
John Cothern
Andy Kho
Norman Lui
Eric Bozeman
Fernando Escobar*

SDSU

San Diego State University

Prof. Antonio Palacios

Grad students

-Susan Guyler
-Huy Vu
-John Aven

OUTLINE

- Motivation
- Potential Applications
- Coupled SQUID/SQIF work
- Coupled Fluxgate
- Other Coupled Devices
- Questions

Motivation

SPAWAR researchers are looking into issues ranging from nonlinear dynamics of sensors, and Microelectromechanical systems (MEMS) to bring about improvements in current systems. The Advanced Dynamics Research group at SPAWAR is globally recognized as one of the premier groups for research in nonlinear dynamics and, possibly, the leading group on practical applications.

This work has led to a compact, cheap and sensitive room temperature magnetometer that the Marine Corps is considering as an intrusion sensor. This talk with feature an overview of how nonlinear science is applied into actual devices and systems.

Potential Applications: Advances in Sensors

- Mine-detection using RUVs or other technique
- Wide area surveillance using large numbers of networked sensors (sensors are compact and cheap…"throw-away") around harbors, choke points, battlefields,etc.
- Bottom or buoy-mounted "tripwire" early-warning system
- Commercial applications: medical scanning, baggage scanning, etc.
- Assorted battlefield applications
- Special military applications
- "Exotica"…coupling fluxgates in a ring: improved sensitivity (SNR), ability to detect cyclic signals, and more…

Location of Sensor

Remote sensors

Mine detectors

Medical imaging System

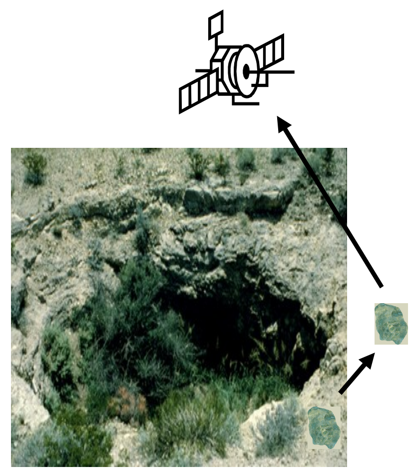

Airport metal detectors

The Co-site Interference Challenge Worsens

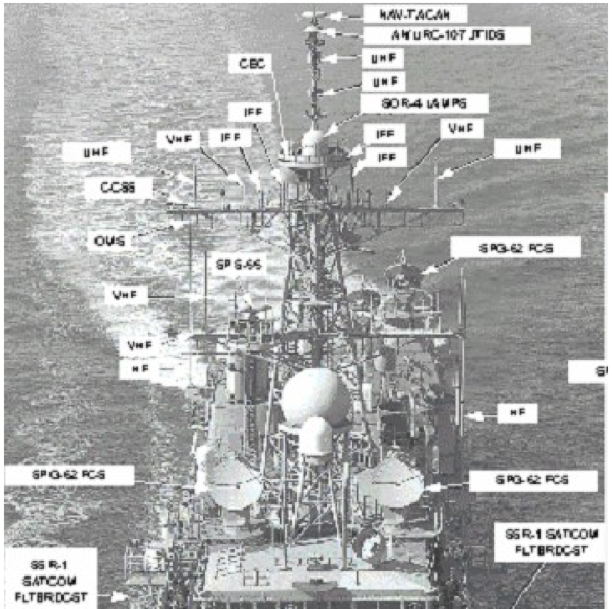

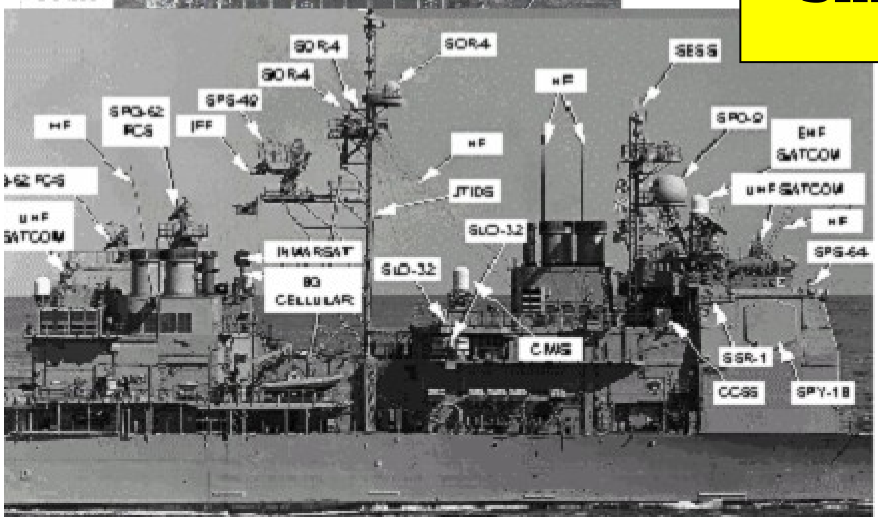

Simplify

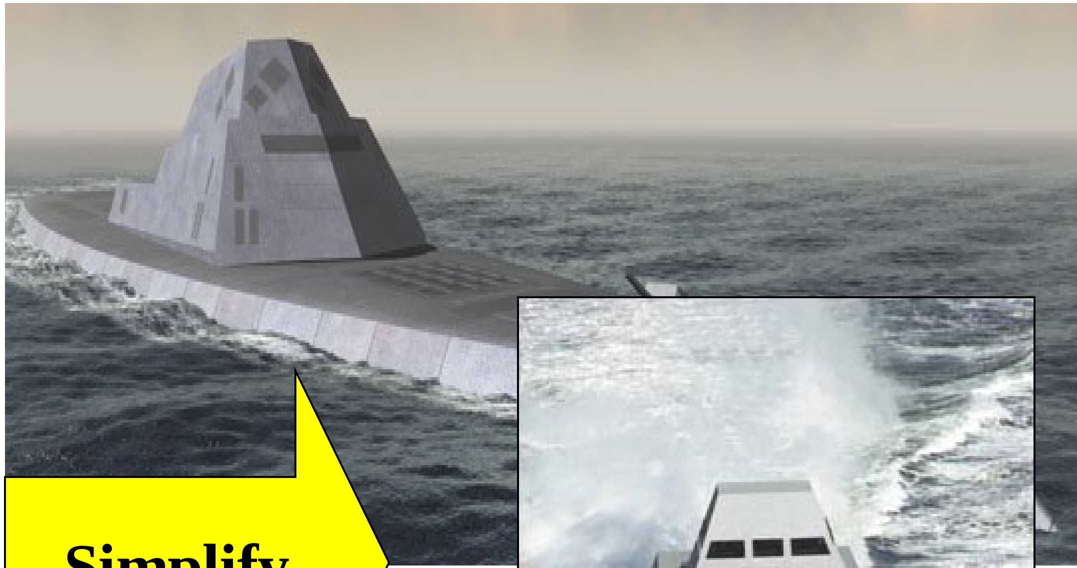

SQUID/SQIF work

Systems Center PACIFIC

Background

Modeling DC SQUID

Using the Josephson relations we can describe the dynamics of the DC-SQUID by the phase difference across the two junctions and arrive at following equations:

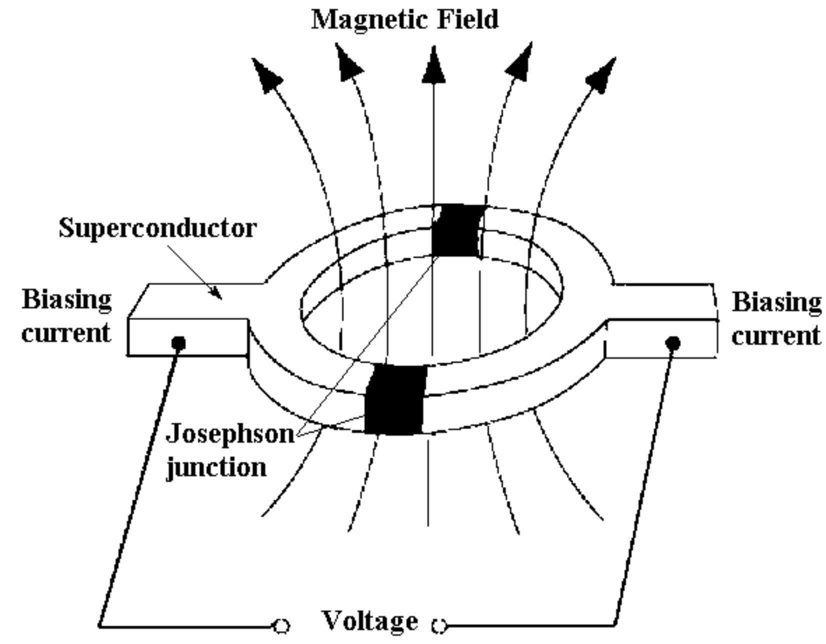

Figure Courtesy of: http://hyperphysics.phy-astr.gsu.edu/hbase/solids/sqzuid.html

$$\tau_\gamma \dot{\delta}_i = J + \frac{(-1)^i}{\beta}(\delta_1 - \delta_2 - 2\pi x_e) - \sin(\delta_i), \quad i = 1, 2.$$

where $\beta = 2\pi L I_0 / \Phi_0$ is the nonlinearity parameter, $\tau_\gamma = \tau / I_0$ is a rescaling of the time constant and $J = I_s / I_0$ is the normalized biased current and $x_e = \Phi_e / \Phi_0$ and is the external flux normalized to the flux quantum.

Dynamics of SQUID array

λ = *Inductive Coupling parameter*

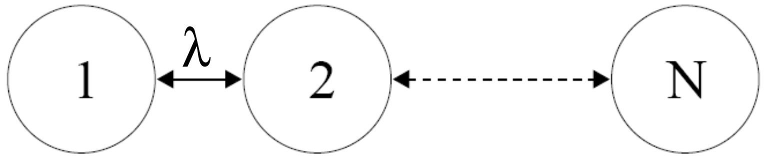

Figure 1: Network of series SQUID array.

The dynamics of the serial SQUID array is described by the following differential equations

$$
\begin{aligned}
\dot{\varphi}_{1j} &= J_1 + (-1)^j/\beta_1(\varphi_{11} - \varphi_{12} - 2\pi x_e + \lambda I_2) - sin(\varphi_{1j}) \\
\dot{\varphi}_{kj} &= J_k + (-1)^j/\beta_k(\varphi_{k1} - \varphi_{k2} - 2\pi x_e + \lambda(I_{k-1} + I_{k+1})) - sin(\varphi_{kj}) \\
\dot{\varphi}_{Nj} &= J_N + (-1)^j/\beta_N(\varphi_{N1} - \varphi_{N2} - 2\pi x_e + \lambda I_{N-1}) - sin(\varphi_{Nj})
\end{aligned}
$$

where

$$I_m = \frac{I_{c,m}}{\beta_m}[\varphi_{m,1} - \varphi_{m,2} - 2\pi x_e]$$

for $j = 1, 2$, and $k = 2 \ldots N-1$, such that N is the number of SQUID loops, λ is the normalized inductive coupling coefficient, and β_k is the nonlinear parameter related to the size of each loop.

DC SQUID Voltage-Flux response (N=1 & 50)

Periodic Voltage Response for Uniform Arrays

N = 1

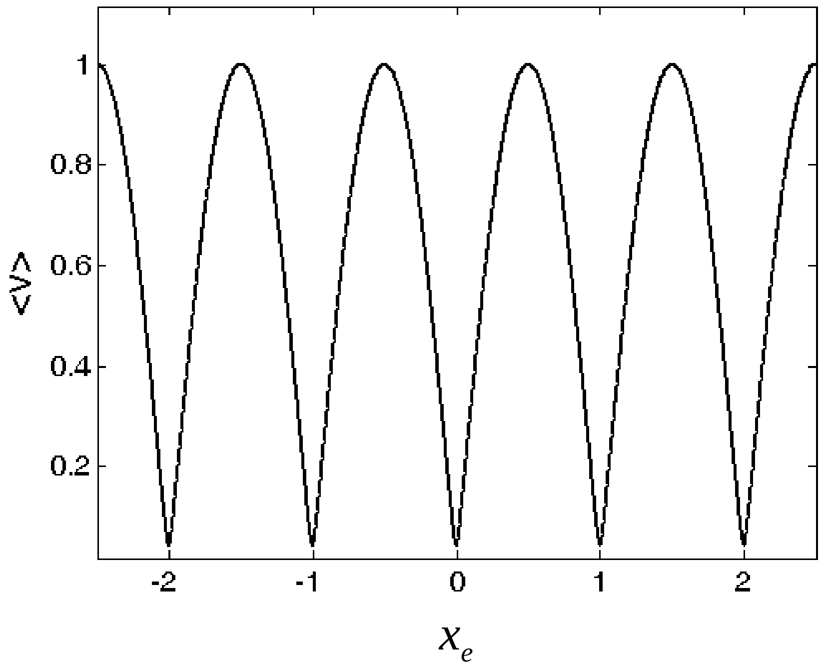

Voltage response vs. the external magnetic field for a uniform SQUID array, where $N = 1$, $\beta = 0.1$, and $I_b = 1.001 I_c$.

N = 50

Series or Parallel (Voltage response similar to single devices)

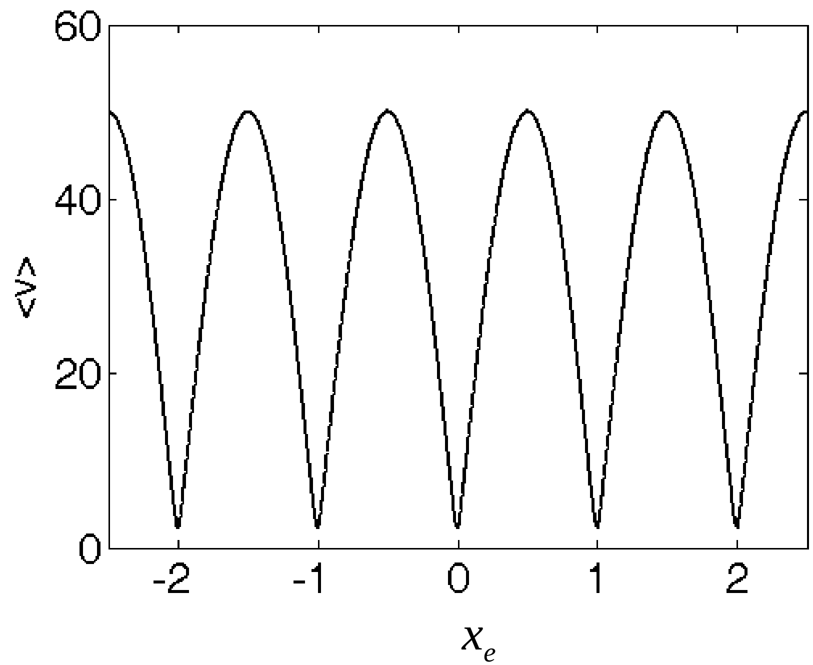

Voltage response vs. the external magnetic field for a uniform SQUID array, where $N = 50$, $\beta = 0.1$, and $I_b = 1.001 I_c$.

1D-SQIFs (variations in loop sizes)

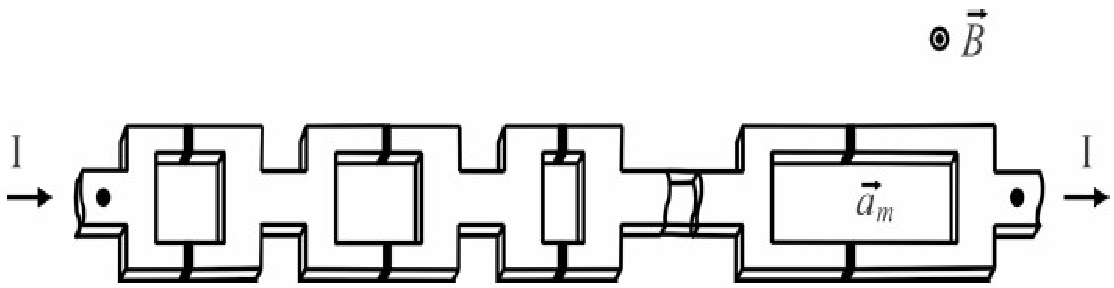

Serial SQUID array

Parallel SQUID array

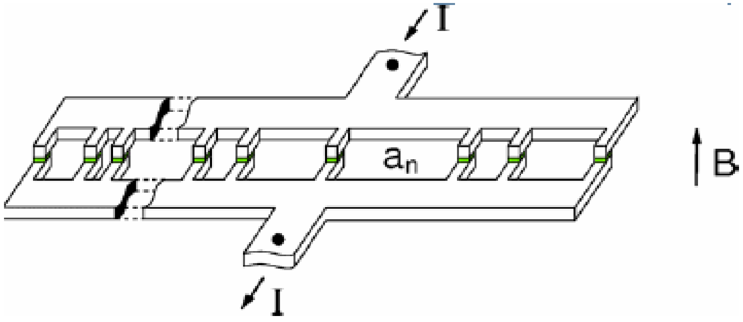

SQIF Voltage Response (N=50)

- Non-uniform SQUID array
- Varying loop sizes
- Anti-peak at zero magnetic field

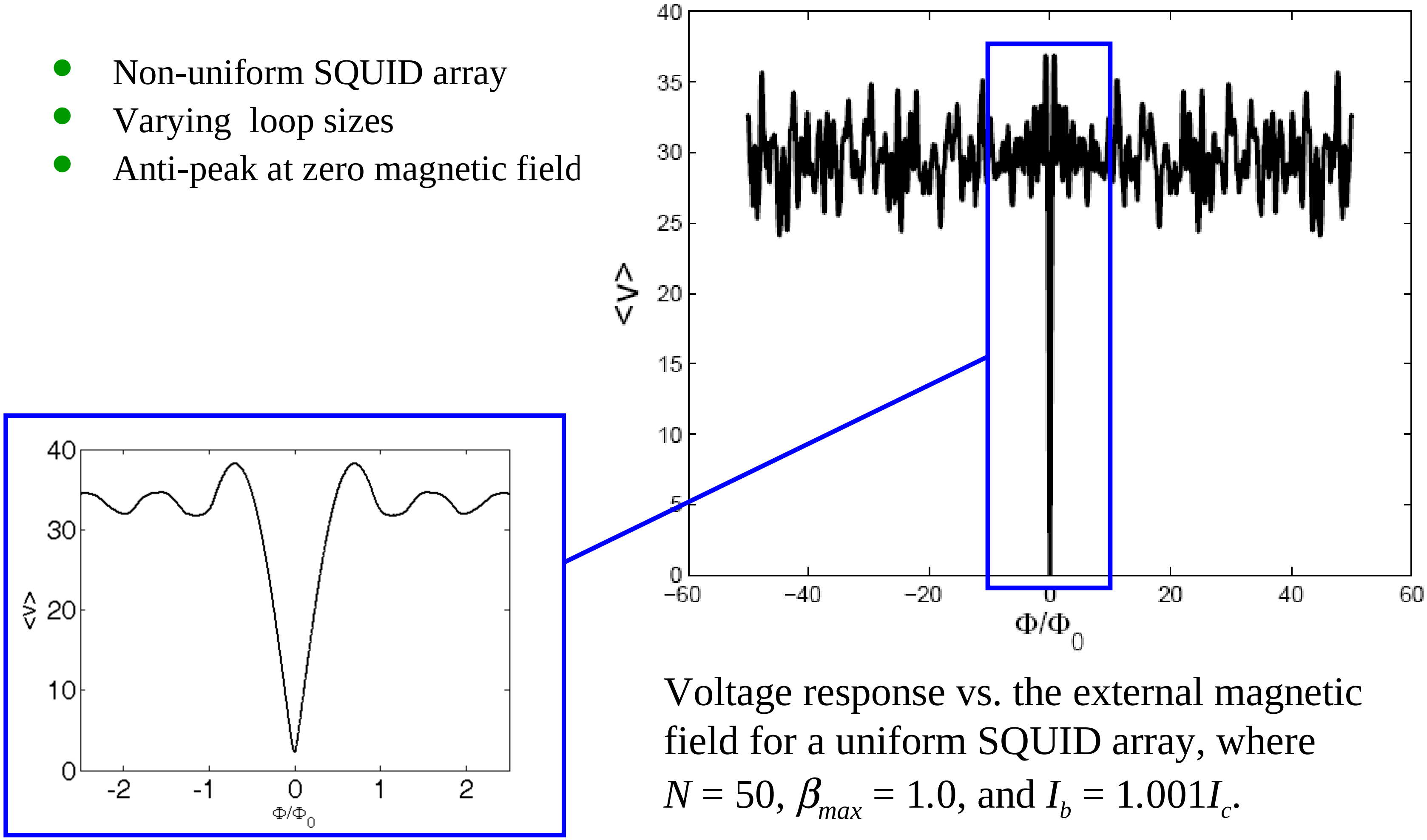

Voltage response vs. the external magnetic field for a uniform SQUID array, where $N = 50$, $\beta_{max} = 1.0$, and $I_b = 1.001 I_c$.

Dynamic Range: Parameter Variation

Increase maximum voltage swing as number of loops (N) increases.

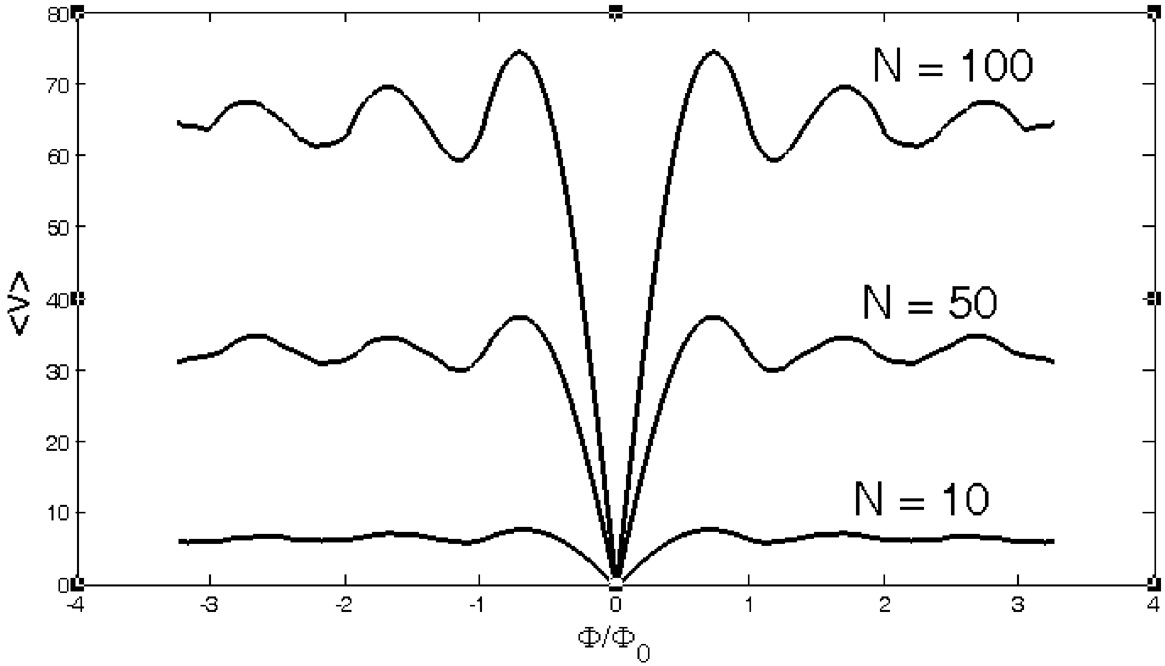

Numerical Computational demand increases as the number of loops increase.

HPC needed for parallelization.

Coupled SQUIDs Theory/Design

THEORY

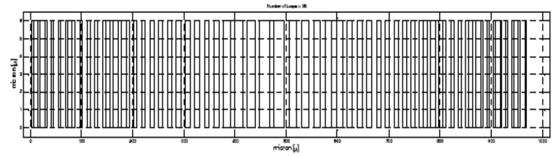

Random Distribution.

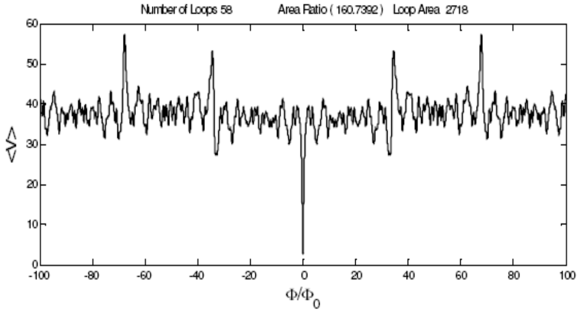

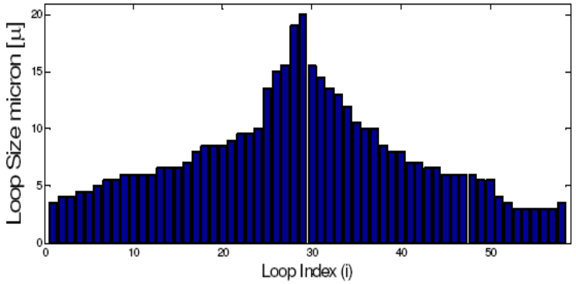

DESIGN

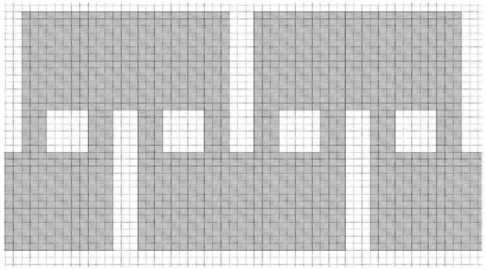

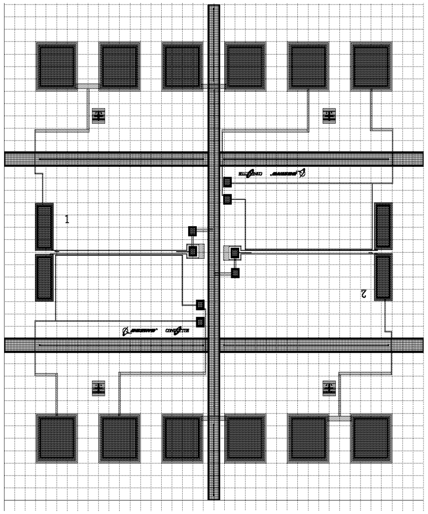

Applied to real world devices that will improve existing technology.

Coupled Sensor Devices

[1] Coupled Fluxgate System
[2] Coupled Bistable Elements: MEMS design
[3] Coupled Array Design
[4] Coupled Systems: Multi-frequency
[5] Locomotion Gaits

[1] Coupled Fluxgate System

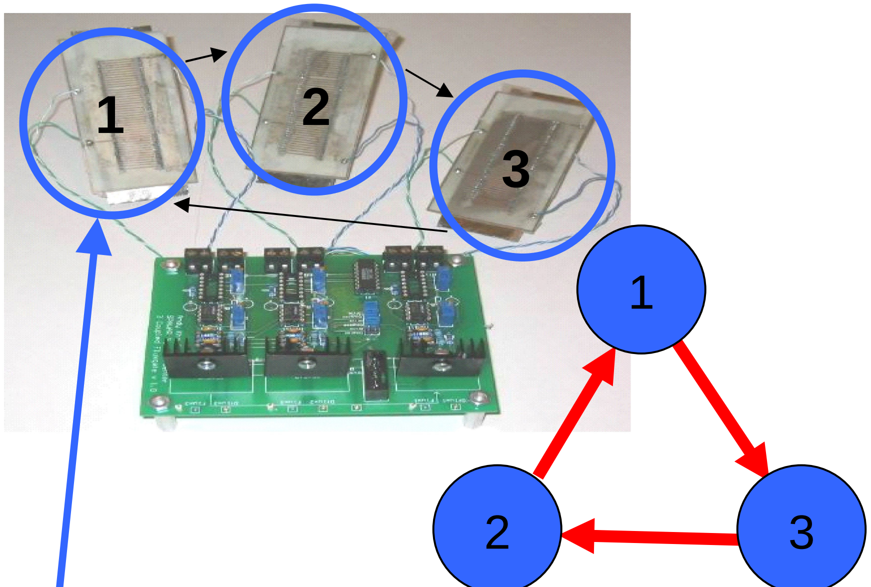

$$\dot{x}_1 = -x_1 + \tanh c(x_1 + \lambda x_2 + \varepsilon)$$
$$\dot{x}_2 = -x_2 + \tanh c(x_2 + \lambda x_3 + \varepsilon)$$
$$\dot{x}_3 = -x_3 + \tanh c(x_3 + \lambda x_1 + \varepsilon)$$

Fluxgate magnetometers are magnetic field sensors used to measure the magnitude and direction of low frequency-dc, low intensity magnetic fields.

Numerical data

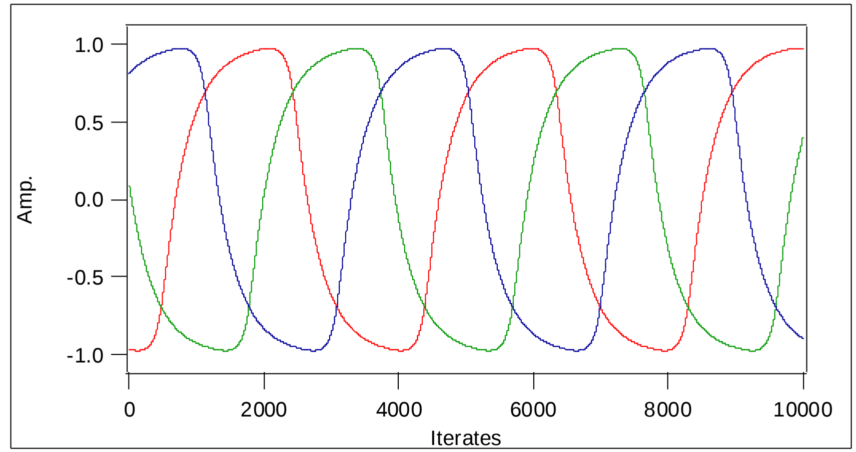

$c = 3$, $\lambda = -1.2$, $\varepsilon = 0.0$

Experimental data showing oscillations

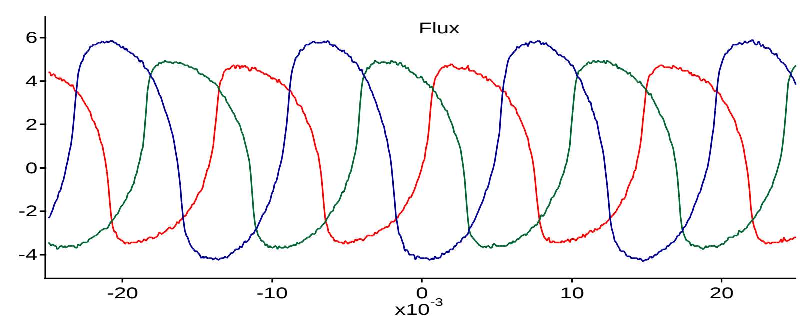

Coupled System: Dynamical Equations

Single Fluxgate

$$\dot{x} = -x + \tanh c(x + f(t) + \varepsilon)$$

f(t) is some periodic forcing function
(square wave, sinusoidal, triangle wave, etc)

Coupled Fluxgates

$$\dot{x}_1 = -x_1 + \tanh c(x_1 + \lambda x_2 + \varepsilon)$$

$$\dot{x}_2 = -x_2 + \tanh c(x_2 + \lambda x_3 + \varepsilon)$$

$$\vdots \qquad\qquad\qquad \vdots$$

$$\dot{x}_n = -x_n + \tanh c(x_n + \lambda x_1 + \varepsilon)$$

N odd

Bifurcation diagram

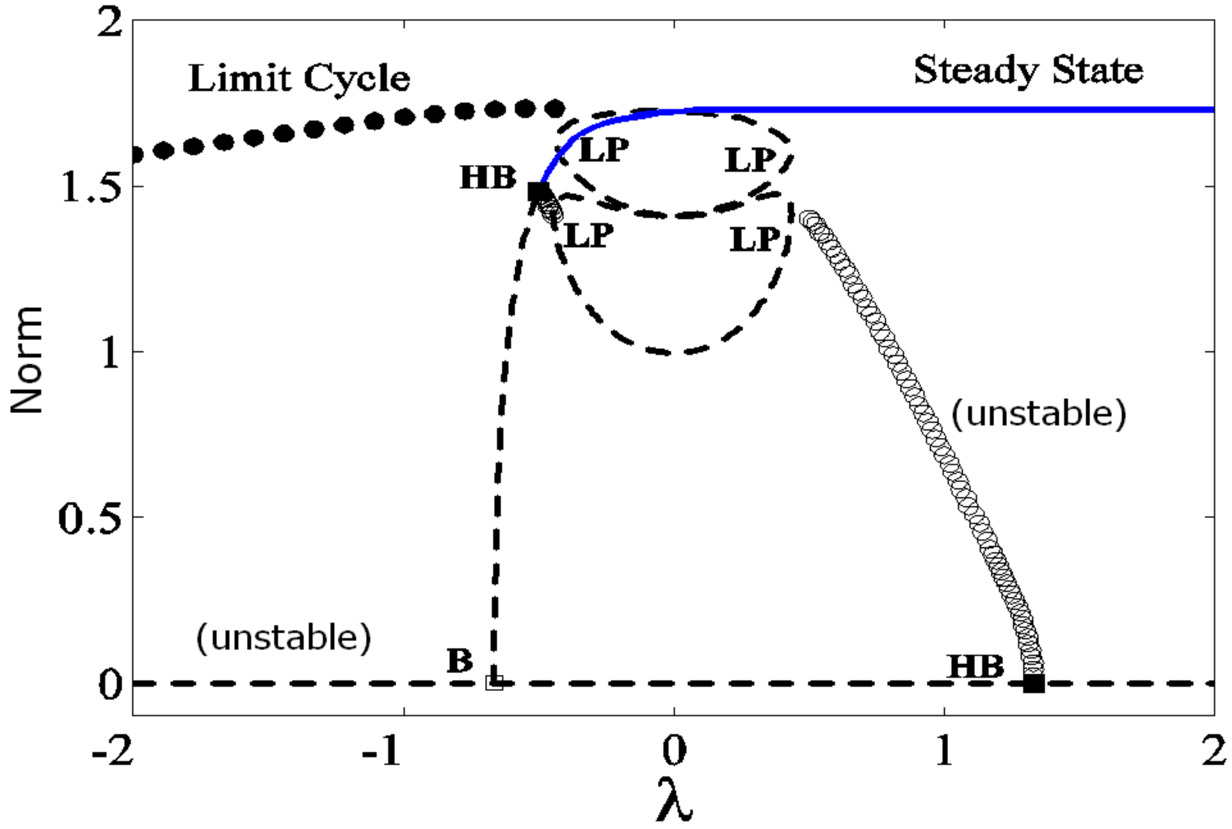

Emergent oscillations in unidirectionally coupled overdamped bistable systems!

Critical value for bifurcation

With much calculations, we derived an expression for the critical coupling strength, λ_c where the bifurcation occurs.

$$\lambda_c = -\varepsilon + \frac{1}{c}\ln\left(\sqrt{c}+\sqrt{c-1}\right) + \tanh\left[\ln\left(\sqrt{c}+\sqrt{c-1}\right)\right]$$

This expression agrees very well with the results obtained from numerical calculations!

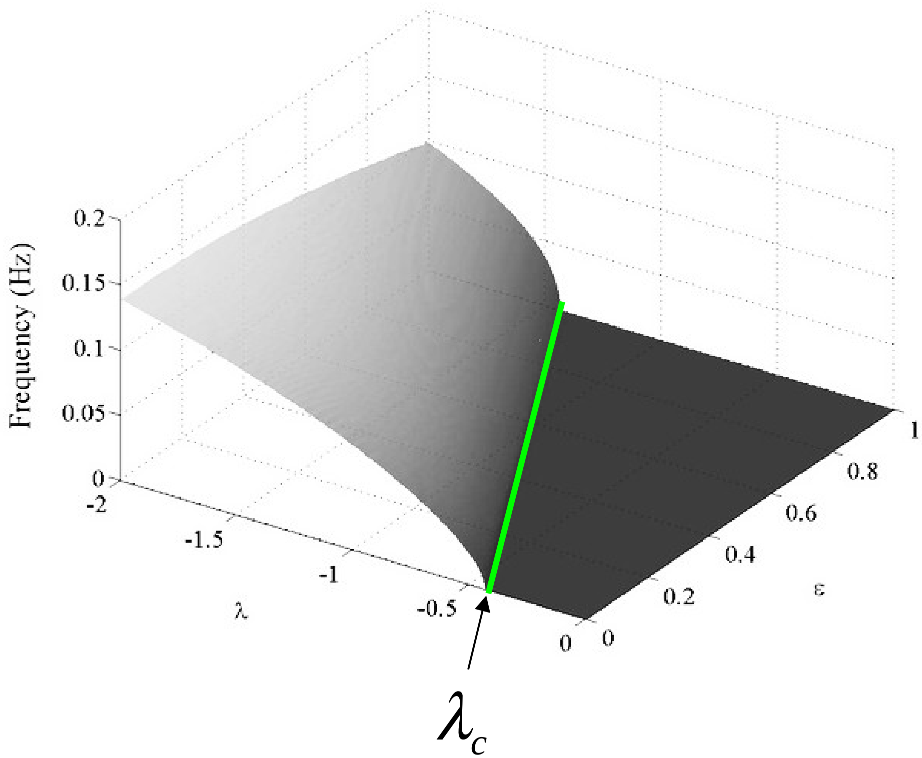

Detection of a ‘target’ signal

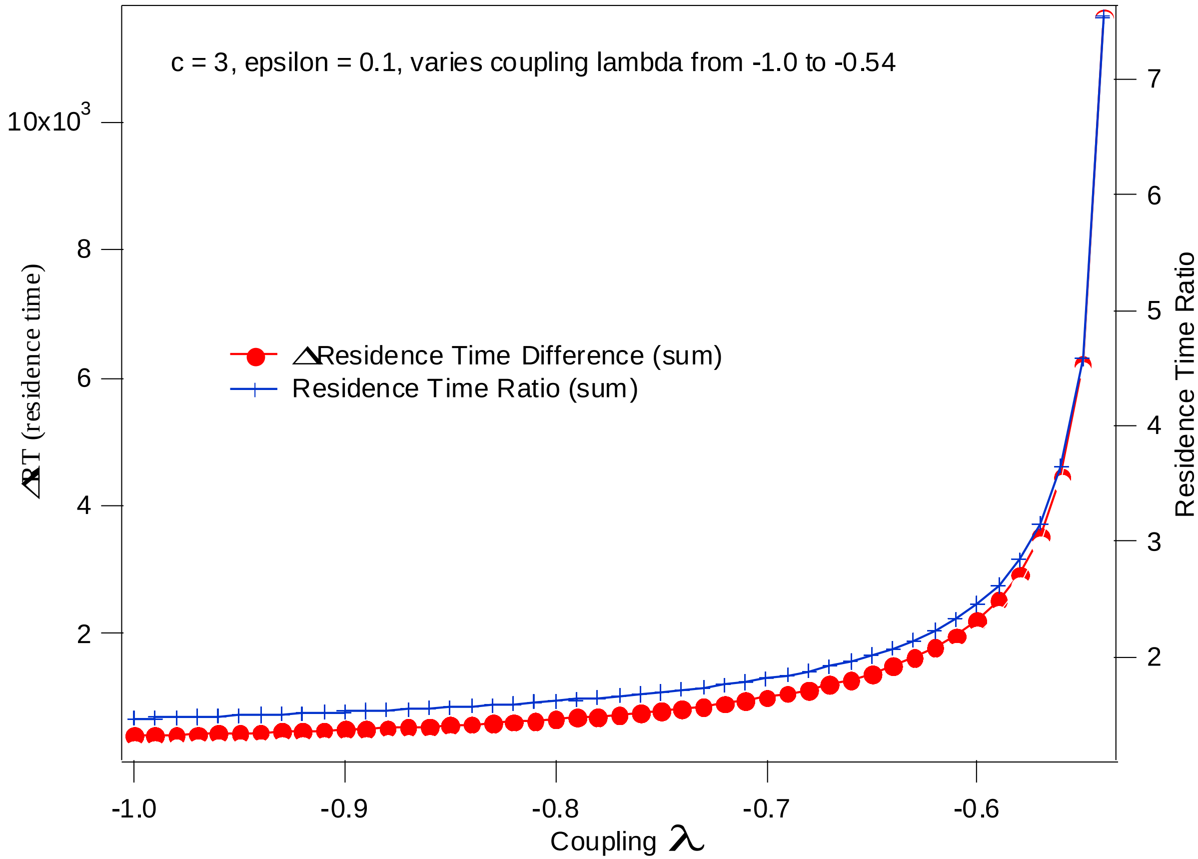

The asymmetry introduced by a “target signal” is *greatly amplified near the onset of the bifurcation* point resulting in great sensitivity of the instrument to resolve the target signal

Applying Incoming Signal to Coupled System

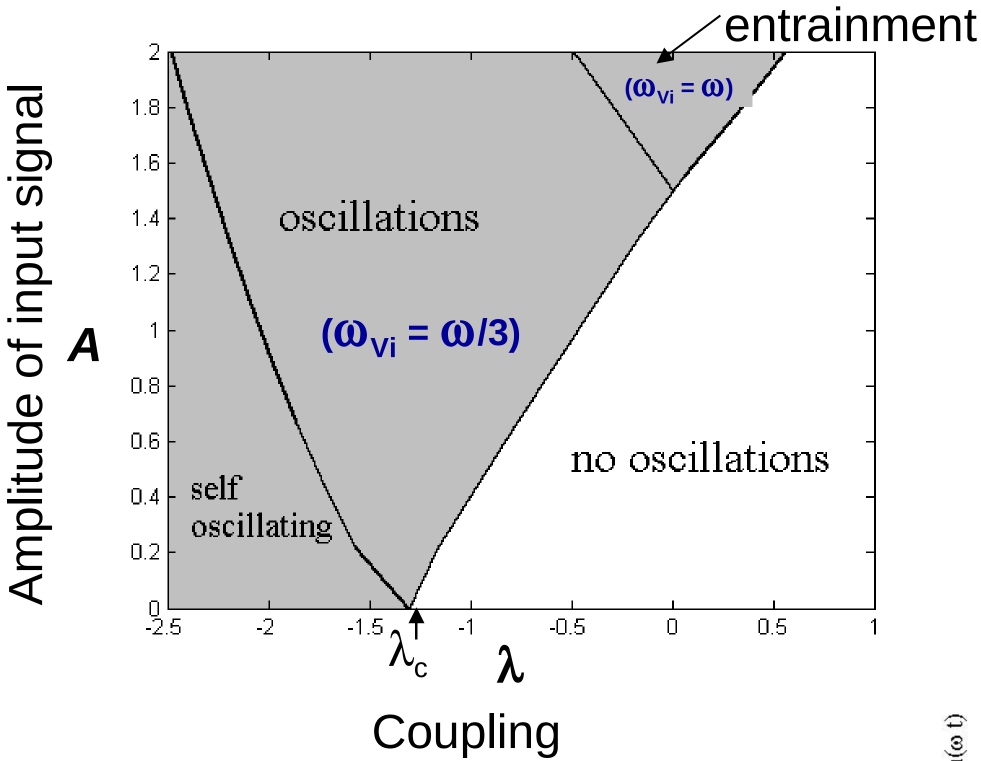

Bifurcation diagram illustrating the different oscillating regions. We are interested in operating the system in the middle region where frequency of each individual element oscillates at 1/3rd the frequency of the incoming signal. ($\omega_{Vi} = \omega/3$.)

Three coupled elements

$$\dot{x}_1 = -x_1 + \tanh c(x_1 + \lambda x_2 + A\sin(\omega t))$$
$$\dot{x}_2 = -x_2 + \tanh c(x_2 + \lambda x_3 + A\sin(\omega t))$$
$$\dot{x}_3 = -x_3 + \tanh c(x_3 + \lambda x_1 + A\sin(\omega t))$$

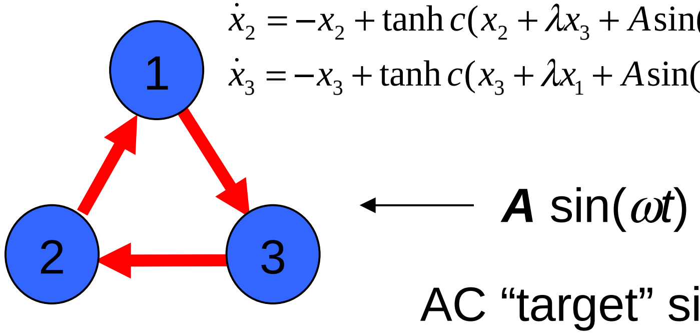

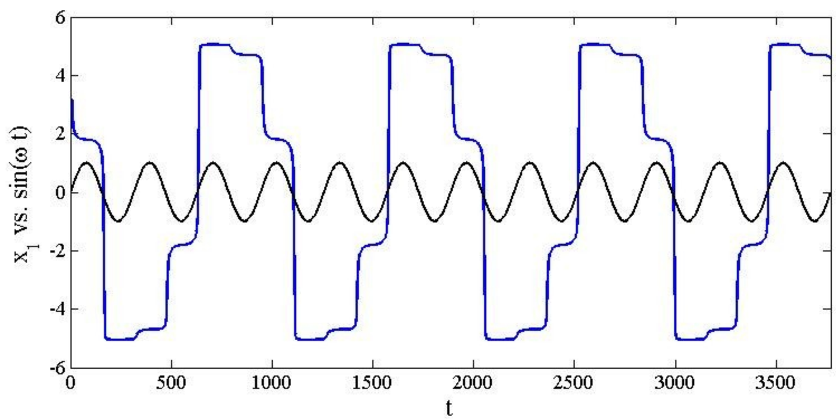

Example of an oscillation at 1/3 the frequency of the incoming signal (black).

[2] Coupled Bistable Elements: MEMS design

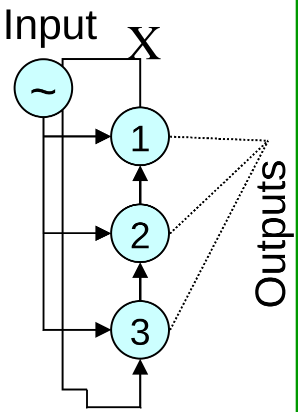

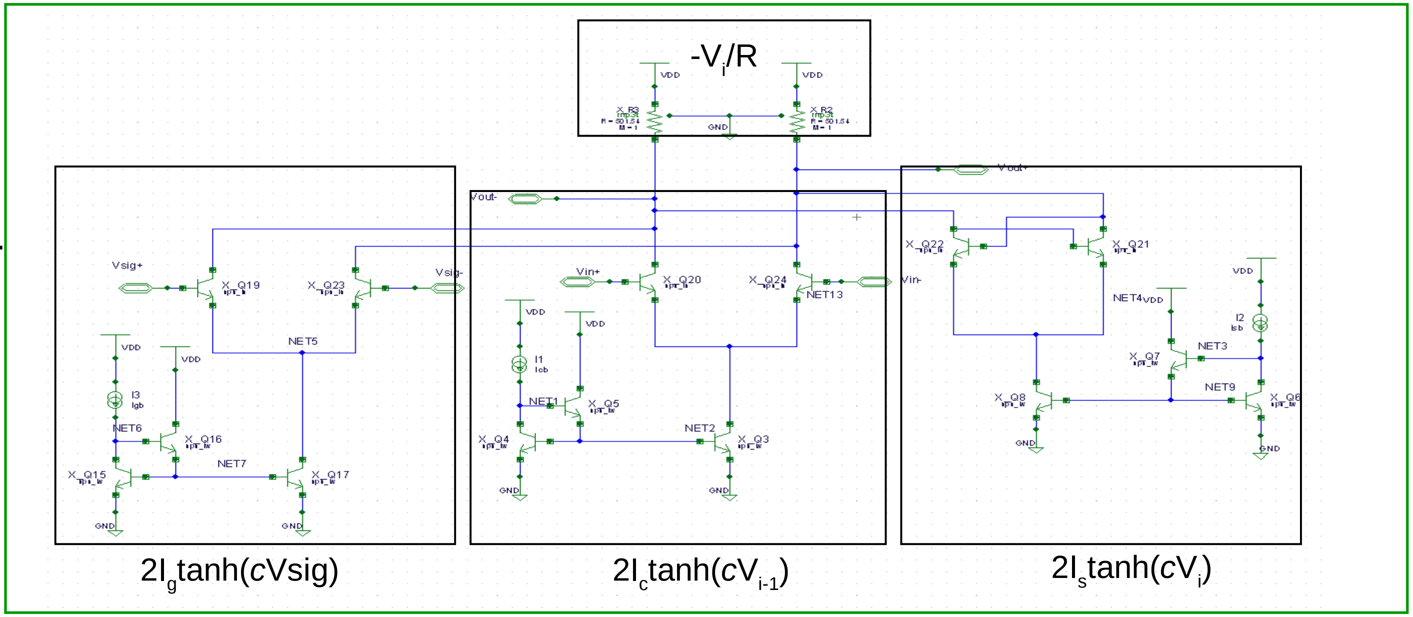

$$C_L \dot{V}_i = -gV_i + I_c \tanh(c_c V_{i-1}) + I_s \tanh(c_s V_i) + I_g \tanh(c_c V_{sig})$$

C_L : Total parasitic capacitance at the output node of the i-th element

V_i : Differential output of the *i*-th element

V_{sig} : Differential input signal

g : Linear conductance

c_c, c_s, c_g : Intrinsic transistor parameter

I_c, I_s, I_g : Bias current

Oscillation: Simulation & Experimental Data

Time series comparison of experimental data vs. simulation data

Simulation Data

Experimental Data

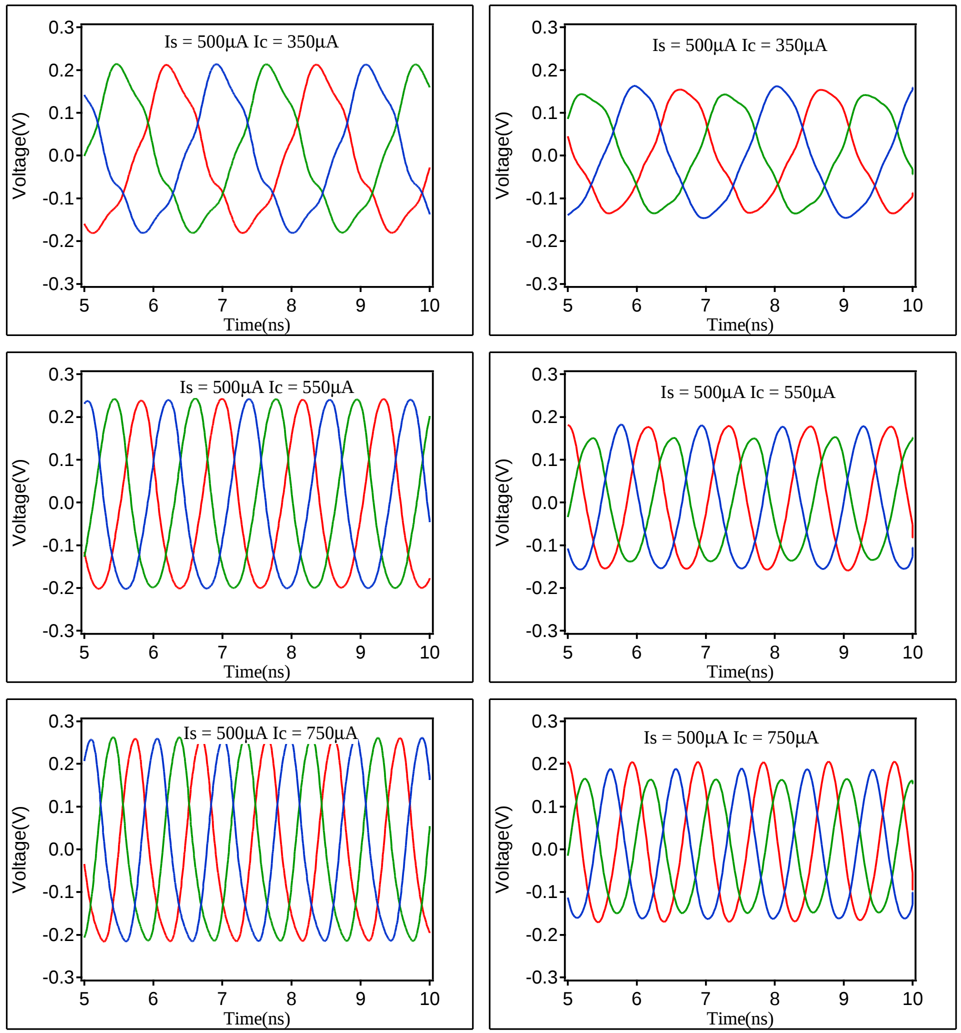

[3] Coupled Array Design

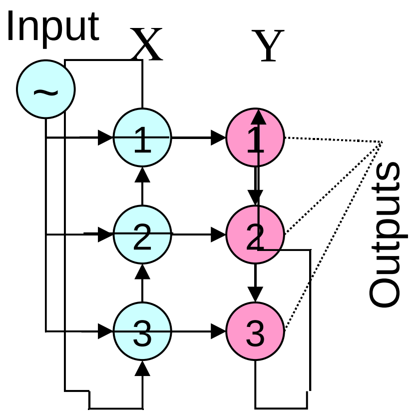

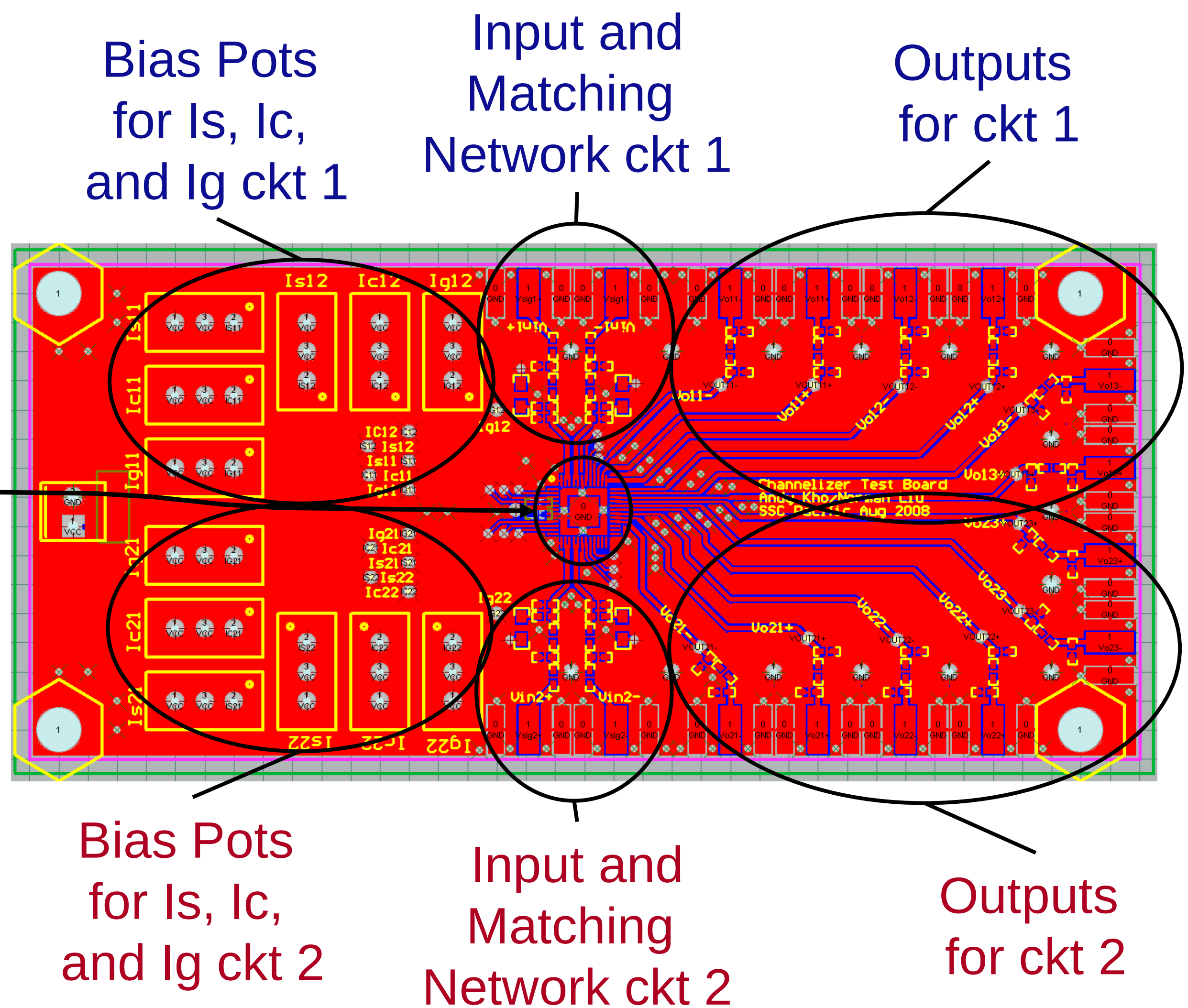

Number of cells	ω_X/ω_Y			
3	2	5	$\cdots$	3k-1
5	4	9	$\cdots$	5k-1
7	6	13	$\cdots$	7k-1
9	8	17	$\cdots$	9k-1
$\vdots$	$\vdots$	$\vdots$	$\ddots$	$\vdots$
N	N-1	2N-1	$\cdots$	Nk-1

The Table represents the down-conversion ratios between the frequency of the X array (first array), and Y array (second array), for a network of two coupled arrays interconnected as is shown in Figure above, where k positive integer.

Results: Coupled Array Design

Numerical Simulation

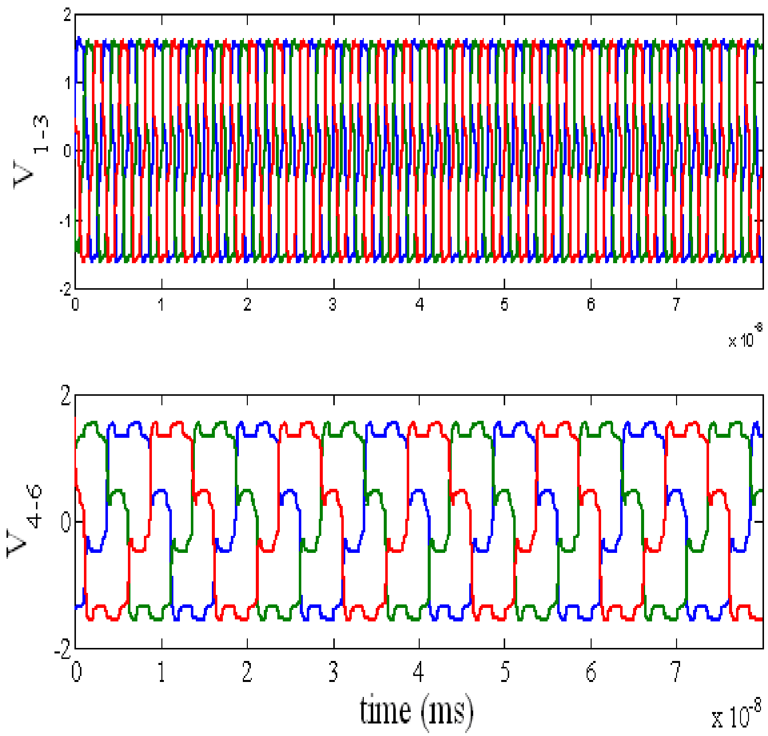

Second array to response at 1/5th the frequency of 1st array.

Experiment

Number of cells	ω_X/ω_Y			
3	2	5	$\cdots$	3k-1

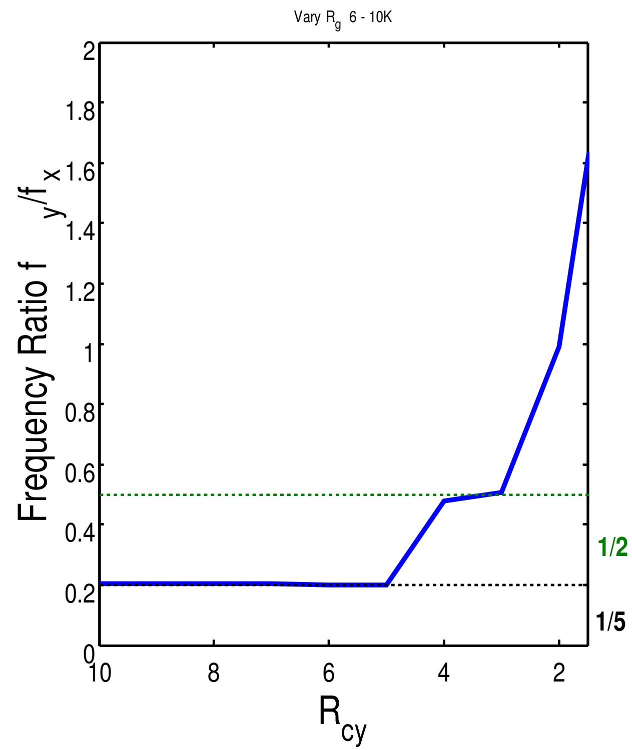

Experimental work demonstrates patterns predicted.

[4] *Coupled Systems: Multifrequency*

Network Connectivity

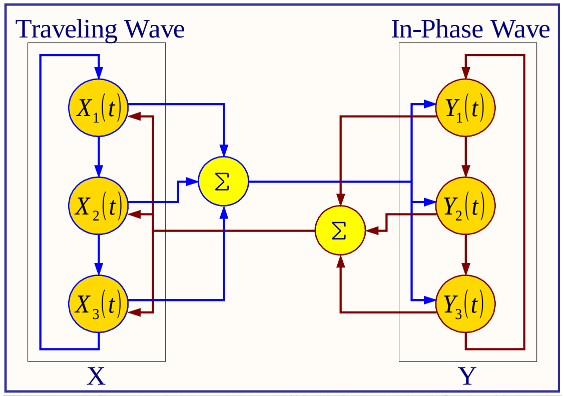

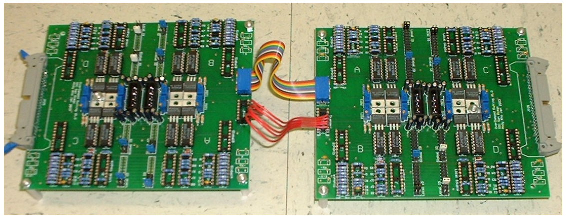

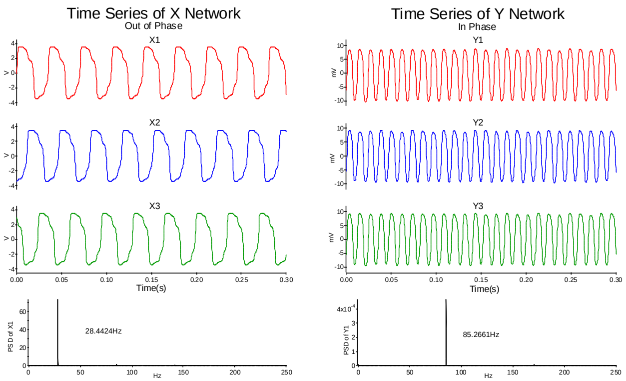

Network Equations

Let the left array be described by

$$\frac{dX_i}{dt} = f\left(X_i\right) + \sum_{j \to i} \alpha_{ij} h\left(X_i, X_j\right)$$

where X_i is the state of cell *i,* h( ) is the coupling function, and a_{ij} is the coupling coefficient.

$$Let\ X(t) = \left(X_1(t), X_2(t), \ldots, X_N(t)\right)$$

be the state of the left array. Similarly the Y-array has the same set up such that the state of the entire network, at any given time, is described by (X(t), Y(t)).

The voltage measurements of the electronic network clearly confirm the finding.

Results for Multifrequency

Numerical Simulation

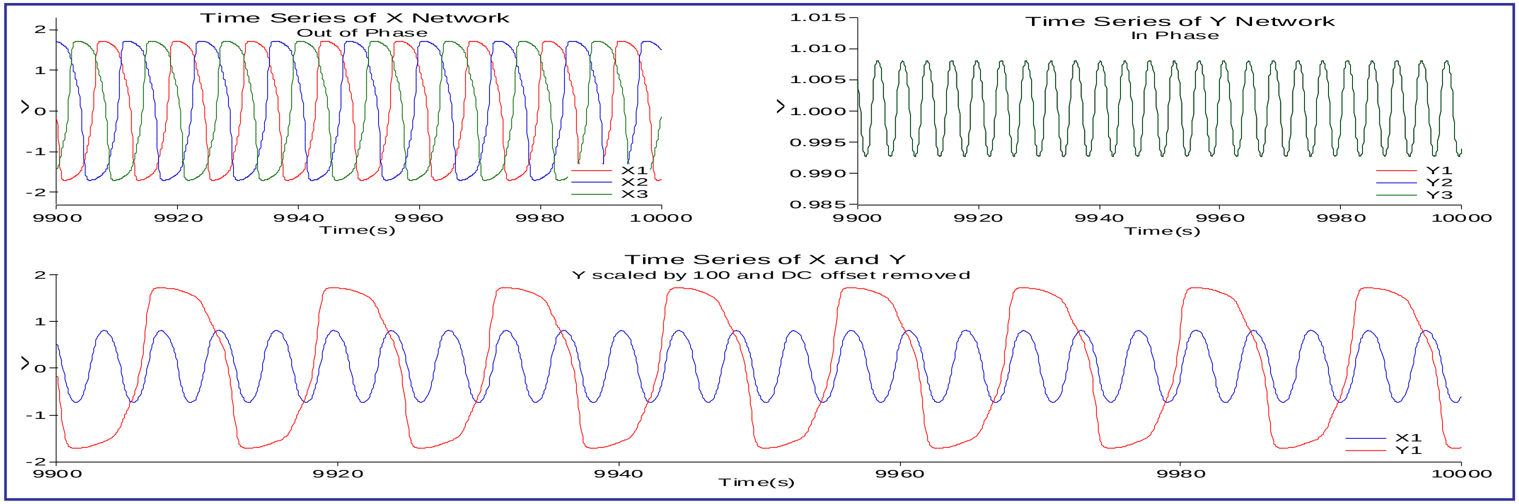

Experiment

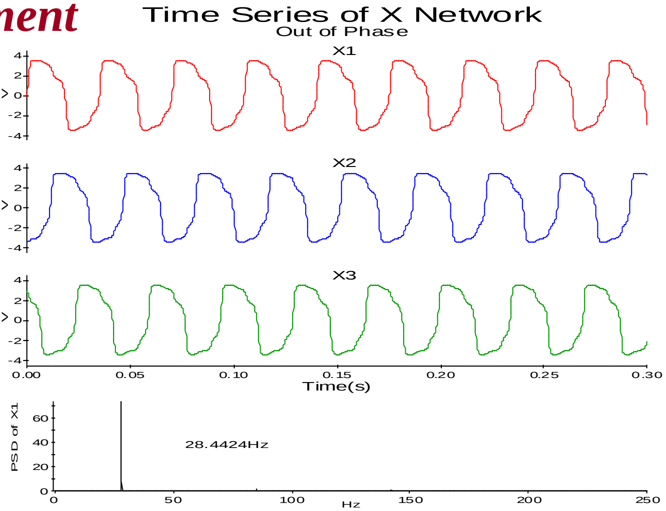

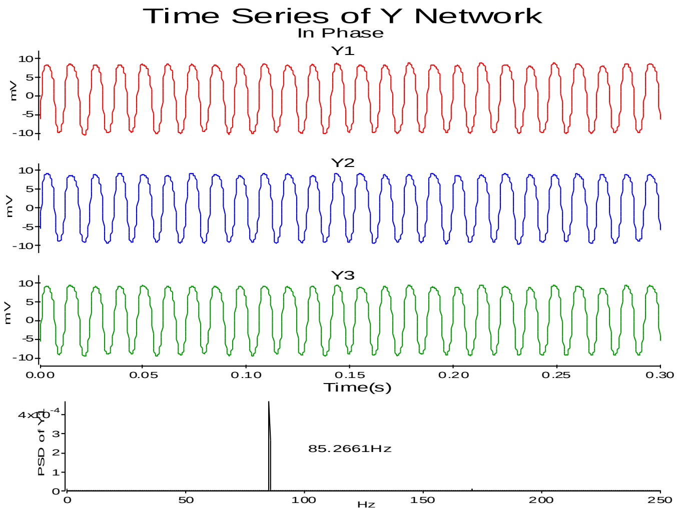

The in-phase pattern is clearly oscillating at three times the frequency of the out-of-phase (traveling wave) pattern.

[5] Locomotion Gaits

Coupling Schematic

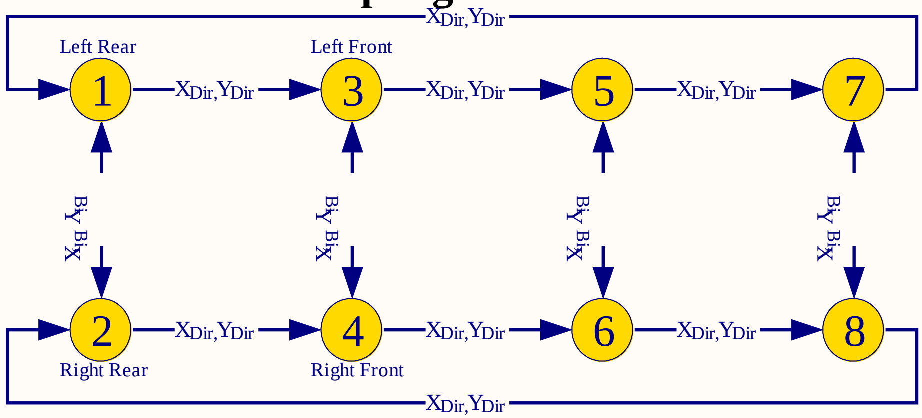

FitzHugh-NagumoNeuron Model

$$\dot{x} = c\left(x + y - \tfrac{1}{3}x^3\right) \equiv f_1(x, y)$$

$$\dot{y} = -\tfrac{1}{c}(x - a + by) \equiv f_2(x, y)$$

$$a = 0.02,\ b = 0.2,\ c = .5$$

Coupling Scheme

$$\dot{x}_i = f_1(x_i, y_i, \lambda) + X_{Dir}(x_{i-2} - x_i) + X_{Bi}(x_{i+\varepsilon} - x_i)$$

$$\dot{y}_i = f_2(x_i, y_i, \lambda) + Y_{Dir}(y_{i-2} - y_i) + Y_{Bi}(y_{i+\varepsilon} - y_i)$$

$$\varepsilon = \begin{cases} +1 & i \text{ odd} \\ -1 & i \text{ even} \end{cases}$$

$i = 1,\ldots, 8$, *the indices are taken modulo* 8

Primary Gaits Created by Hopf Bifurcations

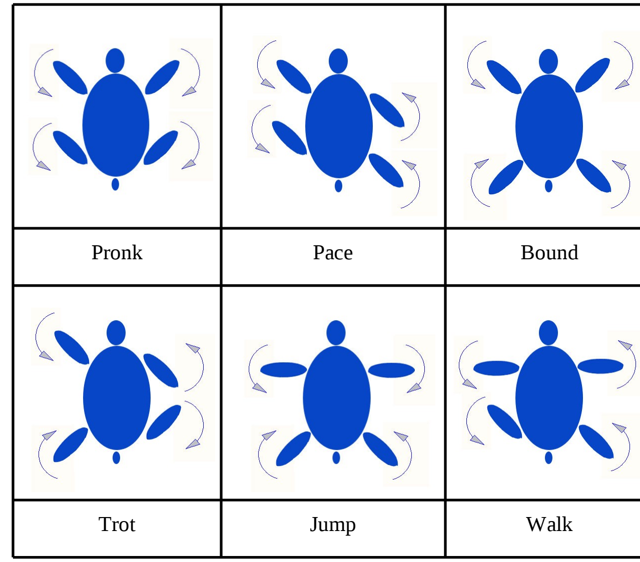

Different gaits are generated by changing the coupling strengths.

Summary of Coupling Signs

Gait	X_{Dir}	X_{Bi}	Y_{Dir}	Y_{Bi}
Pronk	+	+	+	+
Pace	+	-	+	-
Bound	-	+	-	+
Trot	-	-	-	+
Jump	-	+	+	+
Walk	-	-	+	+

Locomotion Gaits (experiment)

Nonlinear Science in Action!

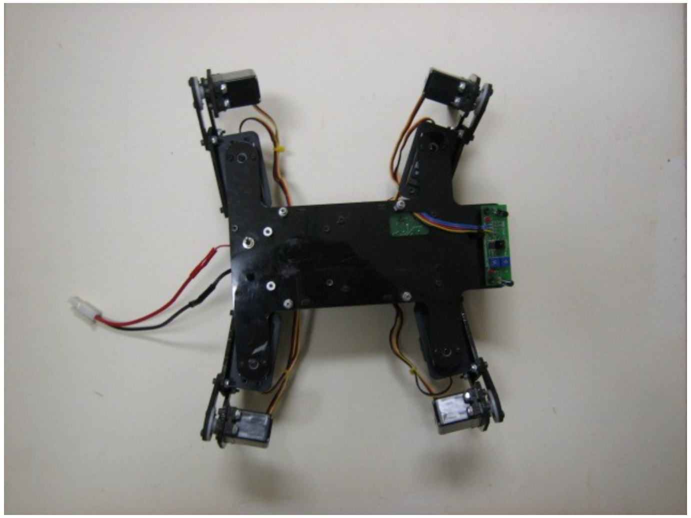

Summary

We have shown with theory and numerical simulations how to take advantage of nonlinear phenomena in order to improve, and design the next generation devices. Our group has many patents, and publications documenting these unique projects. Currently many projects are underway, and the transition to the nonlinear world has begun!

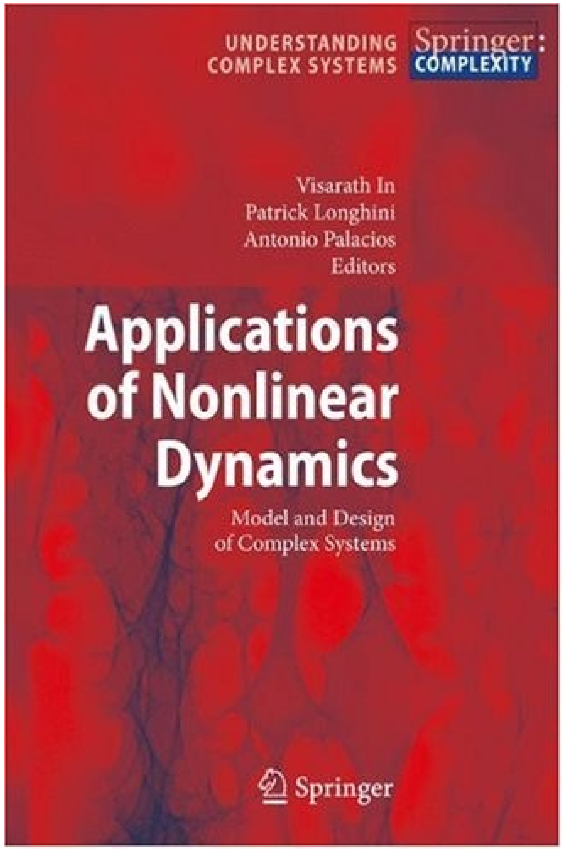

Systems Center PACIFIC

Published Papers

[1] Coupled Fluxgate System
[3] Coupled Array Design
[4] Coupled Systems: Multi-frequency

- **H. Vu, A. Palacios, V. In, P. Longhini, J. Neff. Exploiting Two-time scale analysis of a ring of coupled vibratory gyroscopes. Submitted to Physical Review E (2008).**
- **M. Hernandez, V. In, P. Longhini, A. Palacios, A. Bulsara, and A. Kho . Coupling-induced Oscillations in Nonhomogeneous, Overdamped, Bistable Systems. Physics Letters A, 372, no. 24, 4381-4387 (2008).**
- **A. Bulsara, V. In, A. Kho, A. Palacios, P. Longhini, S. Baglio, and B. Ando. Exploiting nonlinear dynamics in a coupled core fluxgate magnetometer. Measurement Science and Technology 19, 075203 (2008).**
- **[3] P. Longhini, A. Palacios, V. In, J. Neff, A. Kho, and A. Bulsara. Exploiting dynamical symmetry in coupled nonlinear elements for efficient frequency down-conversion Physical Review E 76, 026201 (2007).**
- **A. Palacios, J. Aven,V. In, P. Longhini, A. Kho, J. Neff, and A. Bulsara. Coupled-core fluxgate magnetometer: Novel configuration scheme and the effects of a noise-contaminated external signal. Physics Letters A 367, 25-34 (2007)**
- **V. In, A. Bulsara, A. Kho, A. Palacios, S. Baglio, B. Ando and V. Sacco. Exploiting dynamic cooperative behavior in a coupled-core fluxgate magnetometer. Proceedings of the first Conference of Device Applications of Nonlinear Dynamics. Catania, Italy, 67-82 (2006).**
- **A. Palacios, J. Aven, P. Longhini, V. In, A. Bulsara. Cooperative dynamics in coupled noisy dynamical systems near a critical point; the dc SQUID as a case study. Physical Review E 74, 021122 (2006).**
- **V. In, A. Palacios, A. Bulsara, P. Longhini, A. Kho, Joseph Neff, Salvatore Baglio, and Bruno Ando . Complex behavior in driven unidirectionally coupled overdamped Duffing elements. Physical Review E 73, no. 6, 066121 (2006).**
- **A. Bulsara, J.F. Lindner, V. In, A. Kho, S. Baglio, V. Sacco, B. Ando, P. Longhini, A. Palacios, and W.J. Rappel. Coupling-Induced cooperative behavior in dynamic ferromagnetic cores in the presence of noise. Phsyics Letters A 353 (2006) 4-10.**
- **V. In, A. Bulsara, A. Palacios, P. Longhini, and A. Kho. Complex dynamics in uni-directionally coupled over-damped bistable systems subject to a time-periodic external signal. PRE E 72, no. 4, Rapid Communications 045104 (2005).**
- **A. Palacios, R. Carretero-Gonzalez, P. Longhini, N. Renz, V. In, A. Kho, J. Neff, B. Meadows, and A. Bulsara. Multifrequency synthesis using two coupled nonlinear oscillator arrays. Physical Review E 72, 026211 (2005).**
- **A. Bulsara, V. In, A. Kho, P. Longhini, A. Palacios, W-J. Rappel, J. Acebron, S. Baglio, and B. Ando. Emergent oscillations in unidirectionally coupled overdamped bistable systems. Phys. Rev. E 70, 036103-1-12 (2004).**
- **[4] V. In, A. Kho, J. Neff, A. Palacios, P. Longhini, and B. Meadows. Experimental observation of multi-frequency patterns in arrays of coupled nonlinear oscillators. Physical Review Letters 91, no. 24, (2003) 244101-244101-4.**
- **[1] V. In, A. Bulsara, A. Palacios, P. Longhini, A. Kho, and J. Neff. Coupling-induced oscillations in overdamped bistable systems. Physical Review E 68, Rapid Communication (2003) 045102-1.**

END

Example: Over-Damped Duffing Systems (N=3)

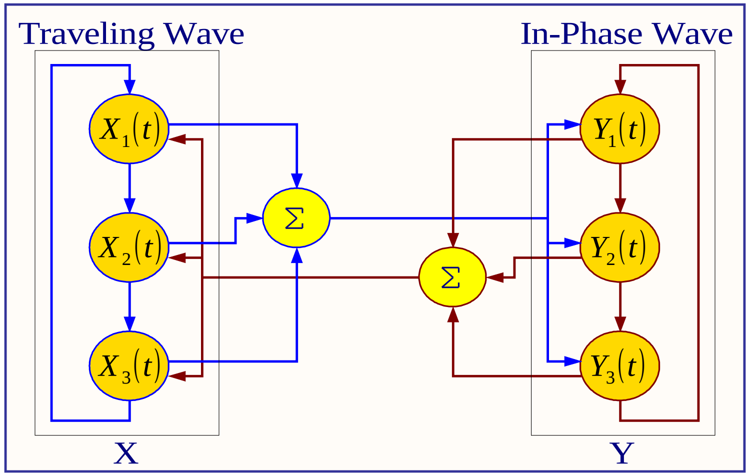

$$\dot{x}_1 = \lambda_x x_1 - x_1^3 + c_x(x_1 - x_2) + c_{xy}\sum_{i=1}^{3} y_i \qquad \dot{y}_1 = \lambda_y y_1 - y_1^3 + c_y(y_1 - y_2) + c_{xy}\sum_{i=1}^{3} x_i$$

$$\dot{x}_2 = \lambda_x x_2 - x_2^3 + c_x(x_2 - x_3) + c_{xy}\sum_{i=1}^{3} y_i \qquad \dot{y}_2 = \lambda_y y_2 - y_2^3 + c_y(y_2 - y_3) + c_{xy}\sum_{i=1}^{3} x_i$$

$$\dot{x}_3 = \lambda_x x_3 - x_3^3 + c_x(x_3 - x_1) + c_{xy}\sum_{i=1}^{3} y_i \qquad \dot{y}_3 = \lambda_y y_3 - y_3^3 + c_y(y_3 - y_1) + c_{xy}\sum_{i=1}^{3} x_i$$

$$c_x = 1, \quad c_y = 1, \quad \lambda_x = 1, \quad \lambda_y = 1, \quad c_{xy} = .02$$